applied sciences

MDPI

Article

Microgravity Induces Transient EMT in Human Keratinocytes by Early Down-Regulation of E-Cadherin and Cell-Adhesion Remodeling

Giulia Ricci [1,2], Alessandra Cucina [2,3,4], Sara Proietti [2,3], Simona Dinicola [2], Francesca Ferranti [5], Marcella Cammarota [1], Antonio Filippini [6], Mariano Bizzarri [2,7,*] and Angela Catizone [2,6,*]

[1] Department of Experimental Medicine, Università degli Studi della Campania "Luigi Vanvitelli", 80138 Naples, Italy; giulia.ricci@unicampania.it (G.R.); marcella.cammarota@unicampania.it (M.C.)
[2] Systems Biology Group Laboratory, Sapienza University, 00161 Rome, Italy; giulia.ricci@unicampania.it (G.R); alessandra.cucina@uniroma1.it (A.C.); sara.proietti@uniroma1.it (S.P.); simona.dinicola@uniroma1.it (S.D.)
[3] Department of Surgery "Pietro Valdoni", Sapienza University of Rome, Via Antonio Scarpa 14, 00161 Rome, Italy
[4] Policlinico Umberto I, viale del Policlinico 155, 00161 Rome, Italy
[5] ASI Agenzia Spaziale Italiana; Via del Politecnico s.n.c. 00133 Roma, Italy; francesca.ferranti@asi.it
[6] Department of Anatomy, Histology, Forensic Medicine and Orthopedics, Section of Histology and Embryology, Sapienza University of Rome, Viale Regina Elena 336, 00161 Rome, Italy; antonio.filippini@uniroma1.it
[7] Department of Experimental Medicine—Sapienza University of Rome, Viale Regina Elena 324, 00161 Rome, Italy
* Correspondence: mariano.bizzarri@uniroma1.it (M.B.); angela.catizone@uniroma1.it (A.C.)

Featured Application: Studies on the effects of microgravity on cell–cell and cell–matrix interaction may help increase the safety and improve the health of astronauts in space.

Abstract: Changes in cell–matrix and cell-to-cell adhesion patterns are dramatically fostered by the microgravity exposure of living cells. The modification of adhesion properties could promote the emergence of a migrating and invasive phenotype. We previously demonstrated that short exposure to the simulated microgravity of human keratinocytes (HaCaT) promotes an early epithelial–mesenchymal transition (EMT). Herein, we developed this investigation to verify if the cells maintain the acquired invasive phenotype after an extended period of weightlessness exposure. We also evaluated cells' capability in recovering epithelial characteristics when seeded again into a normal gravitational field after short microgravity exposure. We evaluated the ultra-structural junctional features of HaCaT cells by Transmission Electron Microscopy and the distribution pattern of vinculin and E-cadherin by confocal microscopy, observing a rearrangement in cell–cell and cell–matrix interactions. These results are mirrored by data provided by migration and invasion biological assay. Overall, our studies demonstrate that after extended periods of microgravity, HaCaT cells recover an epithelial phenotype by re-establishing E-cadherin-based junctions and cytoskeleton remodeling, both being instrumental in promoting a mesenchymal–epithelial transition (MET). Those findings suggest that cytoskeletal changes noticed during the first weightlessness period have a transitory character, given that they are later reversed and followed by adaptive modifications through which cells miss the acquired mesenchymal phenotype.

Keywords: simulated microgravity; focal adhesion; vinculin; E-cadherin; cytoskeleton; HaCaT cells; epithelial–mesenchymal transition (EMT)

Citation: Ricci, G.; Cucina, A.; Proietti, S.; Dinicola, S.; Ferranti, F.; Cammarota, M.; Filippini, A.; Bizzarri, M.; Catizone, A. Microgravity Induces Transient EMT in Human Keratinocytes by Early Down-Regulation of E-Cadherin and Cell-Adhesion Remodeling. *Appl. Sci.* **2021**, *11*, 110. https://doi.org/10.3390/app11010110

Received: 28 October 2020
Accepted: 21 December 2020
Published: 24 December 2020

1. Introduction

Microgravity has noticeable effects at the cellular level, producing morphological and functional alterations in a large number of different cell types [1–4]. It is believed that cellular modifications induced by weightlessness play a fundamental role in the

development of diseases caused by microgravity in astronauts, so in the last decades, it has become crucial to study the effects of simulated microgravity in various experimental models that would mimic different aspects of human physiology [1]. Simulated microgravity can be obtained through the use of various devices. The random positioning machine (RPM) is considered and recognized as a good tool for studying the effects of weightlessness on cell cultures [5].

Studies performed on human epidermal keratinocytes have shown that simulated microgravity exposure induced the modification of expression profiles of several genes in a time-dependent manner and during recovery [6], and it influenced the circadian oscillations of clock genes without affecting either cell proliferation or apoptosis rates [7]. These results underline the existence of an integrated mechanical and chemical signals that influence gene regulation and transcription [8]. In addition, long-term exposure to microgravity conditions is able to affect mouse skin homeostasis [9,10].

In a previous study [11], we have demonstrated that, after exposure to simulated microgravity in random positioning machine (RPM) for 24 h, human immortalized keratinocytes (HaCaT) cells underwent an epithelial–mesenchymal transition (EMT) through the expression of the typical EMT transcription factors and markers. During cutaneous wound healing, the EMT process is necessary to restore the epidermal barrier through re-epithelialization. Keratinocytes surrounding the wound lose their adherent epithelial phenotype and acquire a mesenchymal phenotype [12,13]. Wound re-epithelialization is generally considered a partial and reversible form of EMT [14,15]. In fact, under normal conditions, keratinocytes regain epithelial characteristics when the wound is closed [13]. However, in some pathological conditions, an uncontrolled continued EMT from keratinocytes to myofibroblasts can result in fibrosis [12]. Cutaneous fibrosis, characterized by the accumulation of extracellular matrix components, normally occurs during scar formation in wound repair, but when this process is deregulated and/or accentuated, it can lead to the formation of hypertrophic scars or keloids [16,17]. Therefore, it was extremely important to determine whether the observed effects of simulated microgravity on keratinocytes [11] were constant over time and whether these effects were reversible. These issues are usually left aside by most published studies. Herein, we extend our previous investigation by culturing HaCaT cells in simulated microgravity for up to 72 h to assess their adaptive capability. To evaluate the phenomenon of reversibility, cells subjected to 24 h of microgravity were then cultured under a normal gravitational field (1g) for an additional 24 h. We specifically focused on the maintenance of the EMT phenotype. The migratory phenotype is characterized by cytoskeletal rearrangement and involves new focal adhesion (FA) formation and cell–cell contact disassembling. Vinculin is a key molecule highly expressed in focal adhesion, where it colocalizes with the actin binding layer to facilitate the recruitment of proteins involved in FA dynamics and in the regulation of cell migration. Vinculin is also recruited at cadherin, containing adherents junctions [18], and its activation is sensitive to mechanical stresses, given that focal adhesions (FAs) respond to mechanical forces by inducing conformational changes of the protein [18–21]. Therefore, in order to fully address the study of HaCat cell behavior under simulated microgravity exposure, in this study, we performed confocal and electron microscopy analysis of the junctional features dynamics followed by in vitro migration and invasion assay. Cell samples exposed for short times (24 h) to microgravity show reduced E-cadherin release and impaired its distribution, alongside with dramatic changes in cytoskeleton architecture—involving F-actin filaments and vinculin—that ultimately enhanced cells migratory and invasive properties. As expected, these cells recovered a native morphology, losing their EMT features when replaced into a 1g field. Surprisingly, the same phenomenon—i.e., the EMT reversion—was noticed in cells cultured for longer times (48 and 72 h) in weightlessness. EMT features almost completely disappeared at 72 h, which is when cells display migrating and invasive properties overlapping those values observed in both controls and in cell clusters reseeded into a normal gravity field. Overall, these findings suggest that

EMT is an early and transient effect of weightlessness, given that cells progressively recovered their native morphology and motility phenotype in 48–72 h. Time exposure is a critical parameter that should be carefully considered before conclusive statements could be drawn when performing investigations on living cells cultured in simulated microgravity. Indeed, weightlessness-exposed cells retain the potentiality to reverse to a native phenotype while the epithelial–mesenchymal transition should be viewed as a transitory, adaptive strategy.

2. Materials and Methods

2.1. Cell Culture

The human keratinocytes cell line HaCaT (kindly provided by Prof. MR Torrisi, Sapienza University, Rome, Italy) was cultured in Dulbecco modified Eagle medium (DMEM) supplemented with 10% Fetal Bovine Serum (FBS) and antibiotics (Penicillin 100 IU/mL, Streptomycin 100 μg/mL, all from Euroclone Ltd., Cramlington, UK). The cells were cultured at 37 °C in an atmosphere of 5% CO_2 in air.

2.2. Simulated Microgravity and Cell Exposure

Microgravity conditions were simulated by a Desktop Random Positioning Machine (RPM), which is a particular kind of 3D clinostat [22] manufactured by Dutch Space (Leiden, The Netherlands). The desktop RPM was positioned in a standard incubator. The angular velocity of rotation was set at 90°/s as maximum and 30°/s as minimum in a random mode of the machine. HaCaT cells were seeded into cell culture chambers as described below. Chambers containing HaCaT sub-confluent monolayers were fixed onto the RPM as close as possible to the center of the platform. RPM and 1g cultures were kept in the same humidified incubator at 37 °C in an atmosphere of 5% CO_2 in air.

Cells were placed in RPM for 24 h to investigate the early changes in the morphological and functional phenotype. To assess adaptive process to microgravity, HaCaT cells were placed in RPM for 48 and 72 h. For recovery experiments, HaCaT cells were placed in RPM for 24 h and then transferred into a normal gravitational field for further 24 h.

2.3. Preparation of Cellular Extracts and Western Blot Analysis

HaCaT cells were seeded into cell chambers in a standard medium. Then, cells were serum-deprived for 4 h and, after this time, they were exposed or not to simulated microgravity for adaptation or recovery experiments. At the end of the experimental time, the cells were washed twice with ice-cold PBS (Phosphate-Buffered Saline, Sigma-Aldrich, Saint Louis, MO, USA) and cell pellets were lysed with RIPA buffer (Sigma-Aldrich). A mix of protease inhibitors (Complete-Mini Protease Inhibitor Cocktail Tablets; Roche, Mannheim, Germany) was added just before use. Then, cellular extracts were centrifuged at 8000× *g* for 10 min. The protein content of supernatant fractions was determined by using the Bradford assay. For immunoblot analysis, cellular extracts (40 μg of protein for each sample) were separated on SDS-PAGE gels with a concentration of acrylamide specific for the proteins studied. Proteins were blotted onto nitrocellulose membranes (Bio-Rad Laboratories, Hercules, CA, USA) and probed with mouse anti-E-cadherin C-terminal end monoclonal antibody (BD Transduction Laboratories™, San Diego, CA, USA, Cat# 610181);

Then, the membranes were incubated with the appropriate HRP-conjugated secondary antibody (sheep anti-mouse IgG ECL antibody, GE Healthcare, Little Chalfont, UK, Cat# NA9310) for 1 h at room temperature. Immunocomplexes were detected with an enhanced chemiluminescence kit (Western Bright ECL HRP Substrate, Advansta Inc., Menlo Park, CA, USA) according to the manufacturer's instructions. All Western blot images were acquired and analyzed through Imaging Fluor S densitometer (Biorad-Hercules). Each experiment was performed three times.

2.4. Migration Assay

Cells were incubated at 37 °C with 5% CO_2 under normal gravity conditions (1g) and in microgravity conditions for 24, 48, and 72 h. Migration assay was performed using Cell Culture Insert 12 well 8.0 μm pore size (Falcon, cat.353182, Lincon Park, NJ, USA) placed in a 12 multiwell (Tanswell Falcon, cat. 351143). After the incubation time, the cells were counted and resuspended in DMEM 0.1% FBS. Then, 5×10^5 cells/well were added in the upper chamber of the transwell in DMEM 0.1% FBS, whereas the lower chambers were filled with 800 μL DMEM 10% FBS and incubated for a further 24 h for migration assay.

For recovery experiments, HaCaT cells were placed in RPM for 24 h and then transferred into a normal gravitational field for further 24 h. Then, they were counted and transferred into the upper chamber of the transwell at normal gravitational field for further 24 h for migration assay.

After 24 h of incubation, medium and unmigrated cells in the upper surface of the insert were mechanically removed, and the insert (containing migrated cells in the lower surface) was fixed with paraformaldehyde 4% in PBS (pH 7.4) at 4 °C and staining with Diff Quick solution (DADE, cat. 130832 Network, NJ, USA). Migrated cells were counted under 40× objective using an optical microscope (Axioplan Zeiss Oberköchen, Germany), and the average number ± SD of cells are reported as fold change with respect to control, which is considered as 1. The whole area of each filter was counted. Three independent experiments were performed; each experiment was performed at least in quadruplicate.

2.5. Matrigel Invasion Assay

In vitro invasion assay was performed using chambers coated with GFR Matrigel (Basement Membrane Matrix Growth Factor Reduced, BD Biosciences, cat.354483). The cells were incubated for 24, 48, and 72 h at 37 °C with 5% CO_2 under normal gravity conditions (1g) and in simulated microgravity condition; then, cells were trypsinized, counted, and resuspended in DMEM 1% FBS. Then, 5.0×10^3 cells/well were seeded on the top of the GFR Matrigel in 200 μL of medium 1% FBS, whereas the lower chambers were filled with 800 μL DMEM 10%% FBS. These chambers were incubated for a further 24 h for invasion assay.

For recovery experiments, HaCaT cells were placed in RPM for 24 h and then transferred into a normal gravitational field for further 24 h. Then, they were counted and transferred into the top of GFR Matrigel at normal gravitational field for a further 24 h for invasion assay. At the end of incubation, GFR Matrigel and non-invading cells were mechanically removed with a cotton swab. A polycarbonate filter containing invading cells was fixed with paraformaldehyde 4% in PBS (pH 7.4) at 4 °C. and stained with Diff Quick solution. The filter was analyzed by optical microscope, and four fields/filter were recovered at 10× magnification. Invading cells were counted, and the average number ± SD of cells are reported as fold change with respect to control considered as 1. Three independent experiments were performed; each experiment was performed at least in quadruplicate.

Confocal analysis of GFR Matrigel invasion was done on HaCaT cells dispersed into a single cell suspension; they were labeled using the PKH-26 Red Fluorescent Cell Linker Kit (Sigma-Aldrich, St. Louis, MO, USA), according to manufacturer's instructions.

2.6. Immunofluorescence and F-Actin Localization

Fluorescence analysis was performed in cells grown until semi-confluence. HaCaT cells were cultured into 8-well μ-slides (ibidi GmbH, AmKlopferspitz19, D-82152 Martinsried, Germany) and exposed or not to simulated microgravity for adaptation or recovery experiments as described in "Simulated microgravity and cell exposure section". At the end of incubation, the cells were fixed with 4% paraformaldehyde for 10 min at 4 °C and washed twice for 10 min with PBS. The cells were permeabilized for 30 min using PBS, 3% BSA (Bovine Serum Albumin, Santa Cruz Biotechnology), 0.1% Triton X-100

(Sigma-Aldrich), followed by mouse anti-E-cadherin C-terminal end monoclonal antibody (BD Transduction Laboratories™, Cat# 610181), and mouse anti vinculin (Santa Cruz, Cat sc- 73614 1:50 dilution).

The cells were washed with PBS and incubated for 1 h at room temperature with the secondary antibody (FITC-AffiniPure donkey anti mouse IgG Cat# 715-095-150, RRID: AB_2340792 purchased from Jackson Immuno Research Labs, 1: 200 dilution). TO-PRO3 iodide fluorescent dye 642/661 (1:5000 in PBS, Invitrogen, cat. T3605, Carlsbad, CA, USA) for nuclei staining and rhodamine phalloidin (Invitrogen Molecular Probes Eugene 1:40 dilution) for F-Actin visualization were utilized. Then, the slides were washed with PBS and mounted with 0.1 mM Tris-HCl at pH 9.5: glycerol (2:3). Negative controls were processed in the same conditions besides primary antibody staining. Finally, immunolocalization was analyzed with a Leica confocal microscope TCS SP2 (Leica Microsystems Heidelberg GmbH, Mannheim, Germany) equipped with Ar/ArKr and He/Ne lasers. The laser line was at 488, 543, and 633 nm for FITC, rhodamine, and TO-PRO-3 excitation, respectively. The images were scanned under a 20× or 40× oil immersion objective. E-cadherin quantification was performed using an optical spatial series with a step size of 1 μm. Fluorescence intensity (SUM (I), a.u arbitrary units) was evaluated in sized Regions Of Interest (ROI) that included group of cells. For each ROI, the analyzed cell number was determined counting cell nuclei and the SUM (I) of the ROI was normalized versus the cell number. We counted about 500 cells for each sample. The laser intensity and confocal parameters were maintained at the same values to perform 1g and RPM series. The background threshold of fluorescence was determined by the use of negative control in which the primary antibody was omitted. For depth analyses, an optical spatial series with a step size of 5 μm were recovered. Colocalization analysis was effectuated at the level of periphery of the cell and in an internal compartment at level of cell–cell contact. The fluorescence intensity of vinculin and actin (SUM (I)) at these regions was also quantified. All analyses were performed using Leica Confocal software. Data were analyzed with Sigma Plot Software and Pearson coefficient was used for correlation analysis.

2.7. Transmission Electron Microscopy (TEM) Analysis

Cells cultured as described in the "Simulated microgravity and cell exposure" section were fixed in 2.5% glutaraldehyde in 0.1 M cacodylate buffer (pH 7.4), postfixed in 1% OsO4 in 0.1 M cacodylate buffer, stained with UAR-EMS stain (Electron Microscopy Sciences), de-hydrated in ethanol, and embedded in epoxy resin. Semithin sections were stained with toluidine blue dye. Ultrathin sections (60 nm) were treated with tannic acid and then contrasted with lead hydroxide. Samples were studied and photographed using a Libra 120 Transmission Electron Microscope (Zeiss) equipped with Wide-angle Dual Speed CCD-Camera sharp eye 2 K (4 Mpx) operated by iTEM software (Soft Image System, Münster, Germany).

2.8. Statistical Analysis

Data were expressed as mean ± standard deviation (SD). Data were analyzed with unpaired two-tailed Student's *t*-test or analysis of variance (ANOVA) followed by the Bonferroni post-test. Differences were considered significant at the level of $p < 0.05$. Statistical analysis was performed by using GraphPad Instat software (GraphPad Software, Inc.; San Diego, CA, USA)

3. Results

3.1. E-Cadherin in HaCaT Cells Exposed to Simulated Microgravity

3.1.1. E-Cadherin Expression in HaCaT Exposed to Weightlessness and after Reseeding into a 1g Field

E-cadherin expression was evaluated by Western blot analysis, as shown in Figure 1. In HaCaT cells exposed to simulated microgravity for 24 h, we observed a significant decrease in E-cadherin expression as compared to 1g controls. E-cadherin recovers normal values when the cells were placed in RPM for 48 and 72 h or when HaCaT cells were placed in RPM for 24 h and then transferred into a normal gravitational field for further 24 h (recovery).

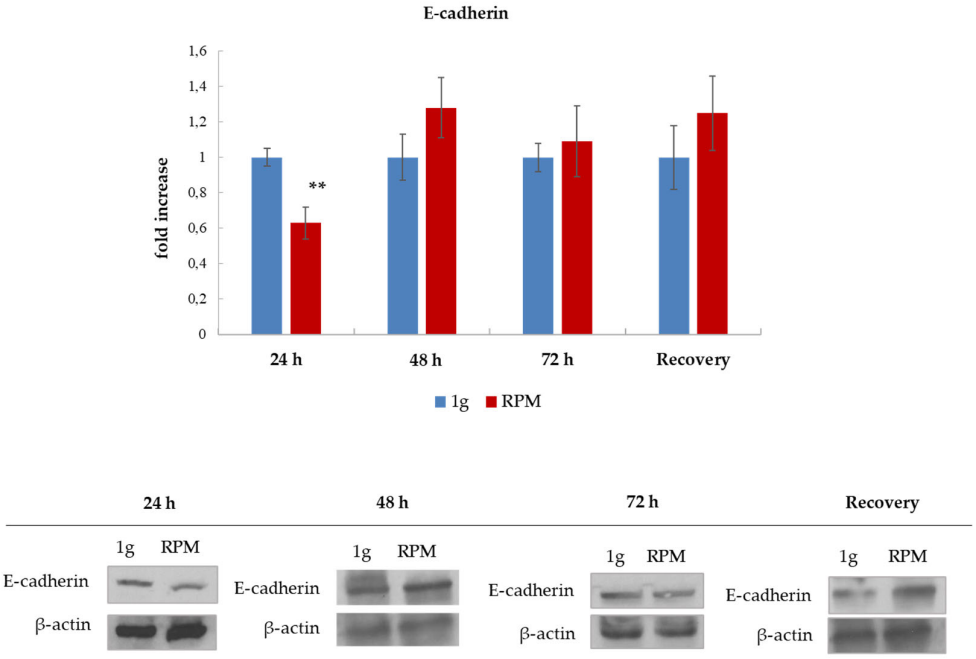

Figure 1. Western blot analyses of E-cadherin in human keratinocytes (HaCaT) cells cultured in normal gravitational condition (1g) and microgravity conditions (random positioning machine, RPM) for 24 h, 48 h, 72 h, and after recovery experiments. Columns represent the densitometric quantification of optical density (OD) of E-cadherin signal normalized with the OD values of ß-actin used as a loading control. Values are expressed as a fold increase of control. Values are means of three independent experiments; SD is depicted as vertical bars ** $p < 0.01$ vs. 1g control by an unpaired two-tailed *t*-test. On the bottom, a panel of representative Western blot analyses is reported.

3.1.2. E-Cadherin Distribution Pattern in HaCaT Exposed to Weightlessness and after Reseeding into a 1g Field

These results are mirrored by data provided by confocal and electron microscopy studies. Indeed, as shown in Figure 2, the fluorescence intensity of E-Cadherin after 24 h in RPM-exposed cells decreases significantly, especially nearby areas of cell-to-cell contact (Figure 2B). To confirm these observations, we performed quantitative analyses of fluorescence intensity, and we found a reduction of about 30% in RPM-treated cells with respect to the 1g condition (128.354 a.u ± 12.654 vs. 178.878 a.u ± 10.522 respectively; $p < 0.01$; Table 1). Moreover, TEM analysis of HaCaT cells evidences well-organized adherens junctions in cell growing at 1g (Figure 2C), whereas a disassembled junctional complex—characterized by a reduced electron density—is noticed in RPM-treated cells (Figure 2D).

For estimating the adaptive process to microgravity, HaCaT cells were placed in RPM for 48 and 72 h and then fixed and prepared for immunofluorescence experiments followed by confocal analysis.

After 48 h of simulated microgravity, intense E-cadherin fluorescence is de novo appreciable within the cell–cell contact area, with only minimal differences when compared to 1g control (Figure 3A,B). At 72 h, both 1g and RPM-exposed cells show a similar distribution pattern of E-cadherin (Figure 3C,D). Overall, these findings suggest that E-cadherin recovers a normal distribution pattern after prolonged exposition to

weightlessness. Similarly, cells maintained in RPM for 24 h and then transferred into a normal gravitational field for a further 24 h recover an E-cadherin distribution pattern that appears undistinguishable from that observed at 1g condition (Figure 3E,F). Moreover, TEM analysis, performed in the same experimental setting, confirms that after 48 h of microgravity exposure, adherent junctions are again observable among cells and present ultrastructural features overlapping with those noticed in cells never exposed to simulated microgravity and growing in a 1g field (Figure 3G,H).

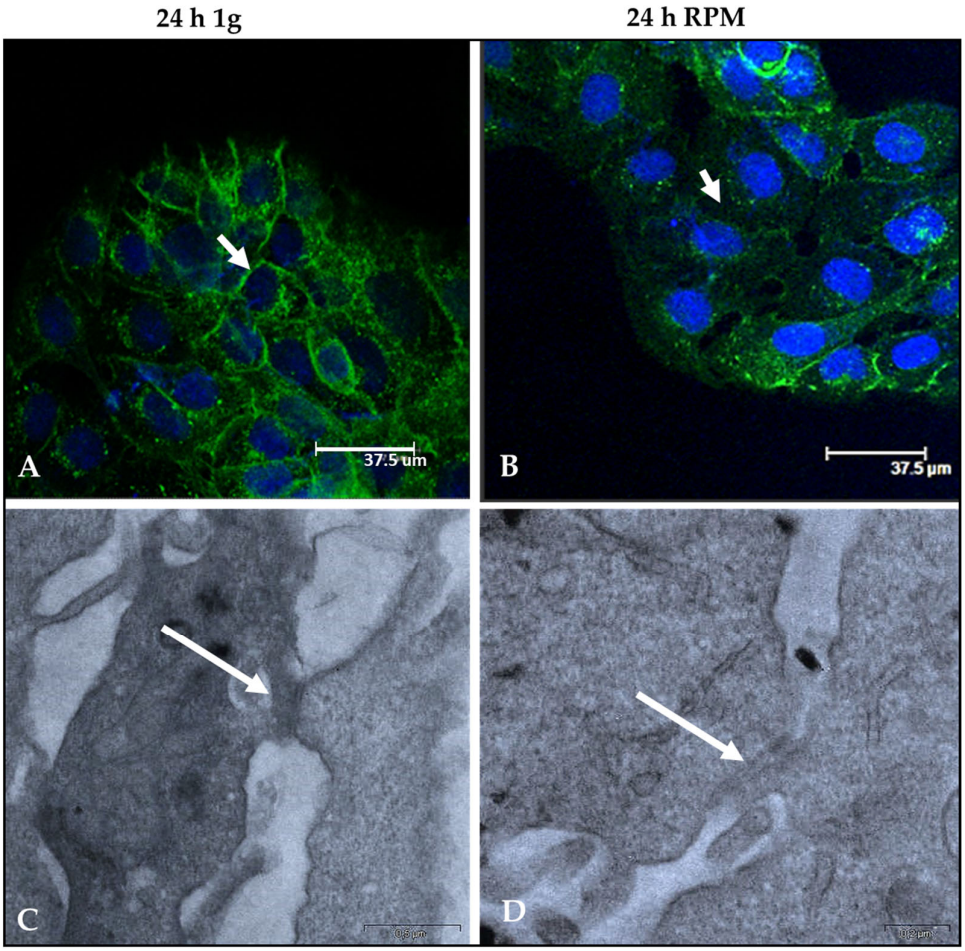

Figure 2. (**A**,**B**) Representative confocal images of E-cadherin distribution pattern in 1g cultured cells (**A**) and RPM cultured cells (**B**) for 24 h. There is an evident decrease of fluorescence intensity (arrows) of E-cadherin after 24 h in microgravity condition particularly at cell–cell contact with respect to the 1g condition. Scale bars 37.5 µm. (**C**,**D**) representative TEM images of cells cultured in the same conditions of A and B respectively. Arrows indicate cell–cell contacts. Magnification 10,000×.

Table 1. Quantitative analysis of fluorescence intensity of E-cadherin. Fluorescence intensity (SUM (I), a.u arbitrary units) was evaluated in about 500 cells. (S.E. Standard Error; 24 h 1g vs24 h RPM $p < 0.01$ valuated by Student's *t*-test).

	24 h 1g	24 h RPM
Fluorescence intensity ((SUM (I) a.u./cell)	178.878 ±10.522 S.E.	128.354 ±12.654 S.E.
Cell number	500	504

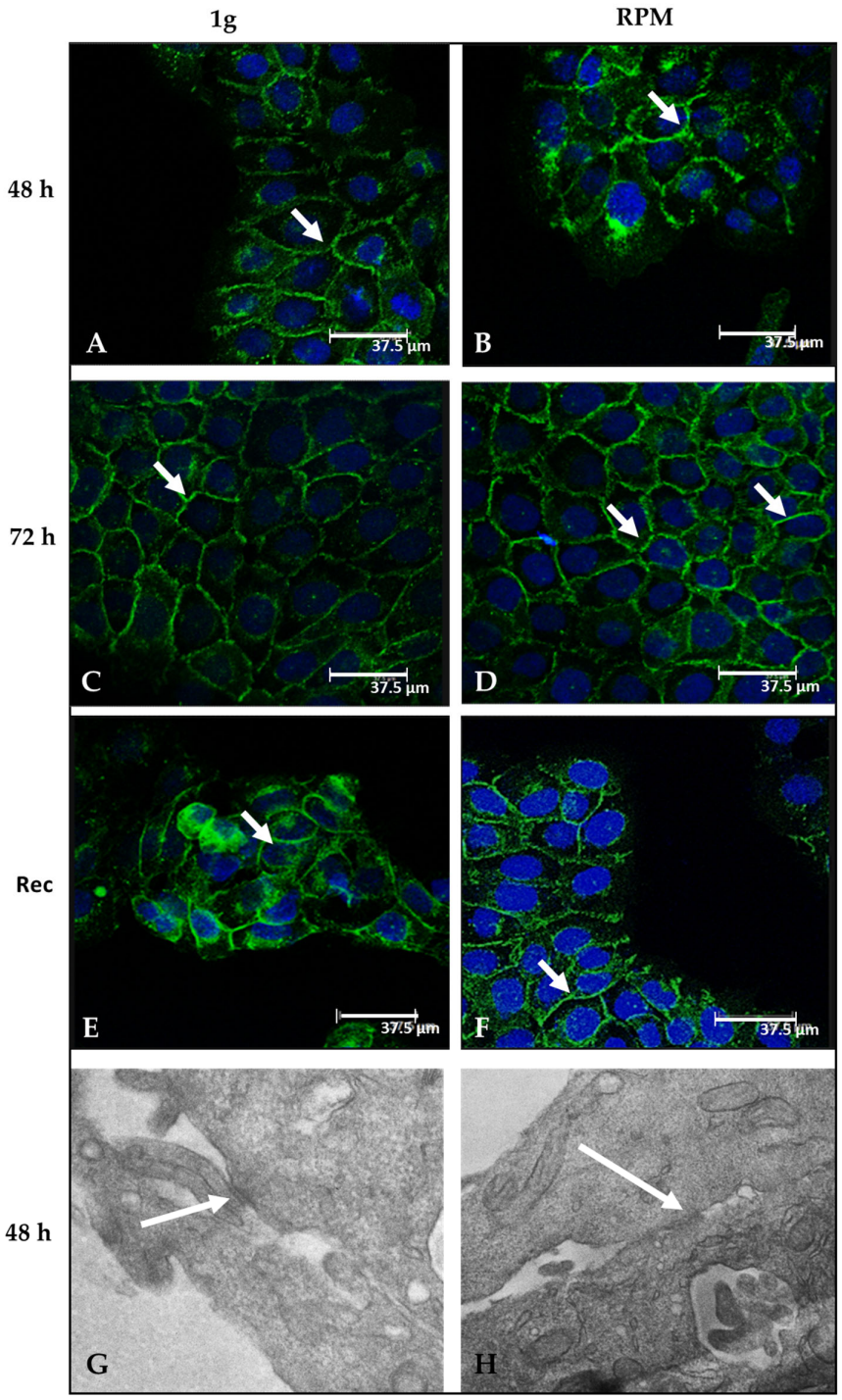

Figure 3. Representative confocal images of E-cadherin distribution in 1g (**A**,**C**) and RPM cultured cells for 48 and 72 h (**B**,**D**); (**E**) Control condition at 1g for 48 h; (**F**) recovery conditions: HaCaT cells were placed in RPM for 24 h and then transferred into a normal gravitational field for further 24 h. Under these conditions, E-cadherin fluorescence is again appreciable within the cell–cell contact area with a similar distribution pattern to the 1g condition (arrows). Scale bars 37.5 µm. (**G**) H representative TEM images of cells cultured for 48 hours at 1g (**G**) and in RPM condition (**H**). Arrows indicate cell–cell contact. Magnification 10,000×.

3.2. Cytoskeleton Modifications of HaCaT Exposed to Simulated Microgravity

To assess the cytoskeleton reorganization occurring in keratinocytes exposed to simulated microgravity for 24, 48, and 72 h, we investigated changes involving the distribution pattern of F-actin and Vinculin, which is a molecule that is highly expressed in focal adhesion, and it is also recruited at cadherin containing adherents junctions [18].

3.2.1. F-Actin and Vinculin Organization after 24 h of Simulated Microgravity

As we described in a previous paper [18], cells cultured in 1g for 24 h showed F-actin distributed in peripheral cortical bundles, while in simulated microgravity exposed cells, a relevant increase of lamellipodia, filopodia, and ruffles were frequently observed. Overall, those findings suggest that cells exposed to weightlessness acquire a motile/invasive phenotype.

To obtain further morphological insights, we performed confocal analysis of the cell to recognize how vinculin colocalizes and correlates with actin filament in shaping FAs, which plays a pivotal role in modulating cell adhesion to the substrate and, henceforth, cell migration. The colocalization analysis and fluorescence intensity of vinculin and actin (SUM (I)) at the free front of the cell membrane, and in an internal compartment at the level of cell–cell contact was performed as described in the Materials and Methods section. As shown in Figure 4A, in control condition, vinculin is predominantly distributed nearby the cell–cell contacts. Colocalization and correlation analyses showed a few or no colocalization of vinculin with actin at the leading edge of the cell culture (Figure 4C) and no significant positive relationship. ($r = 0.174$ $p > 0.05$). In addition, in cell contact, there is no significant relationship between F-actin and vinculin ($r = 0.29$ $p > 0.05$), although these two proteins are tightly associated (at a few points, the cellular contacts colocalize), as indicated in the green and red picks in the figure (Figure 4E). After 24 h of exposure to weightlessness, vinculin was mostly displaced at the cell periphery, and it showed an increased density in the newly formed ruffles and filopodia (Figure 4B). Colocalization and correlation analyses demonstrate that vinculin colocalizes with actin filament at the level of membrane protrusions (Figure 4D), and the correlation coefficient revealed a positive relationship between these two markers ($r = 0.97$; $p < 0.001$), indicating the presence of FA. By contrast, both colocalization (Figure 4F) and the association between F-actin and vinculin decrease at the site of cell adhesion contacts, and there is no significant positive relationship ($r = 0.29$ $p > 0.05$) between the two markers. These results confirm the formation of new FAs necessary to the acquisition of the motile/invasive phenotype by the cells exposed to simulated microgravity.

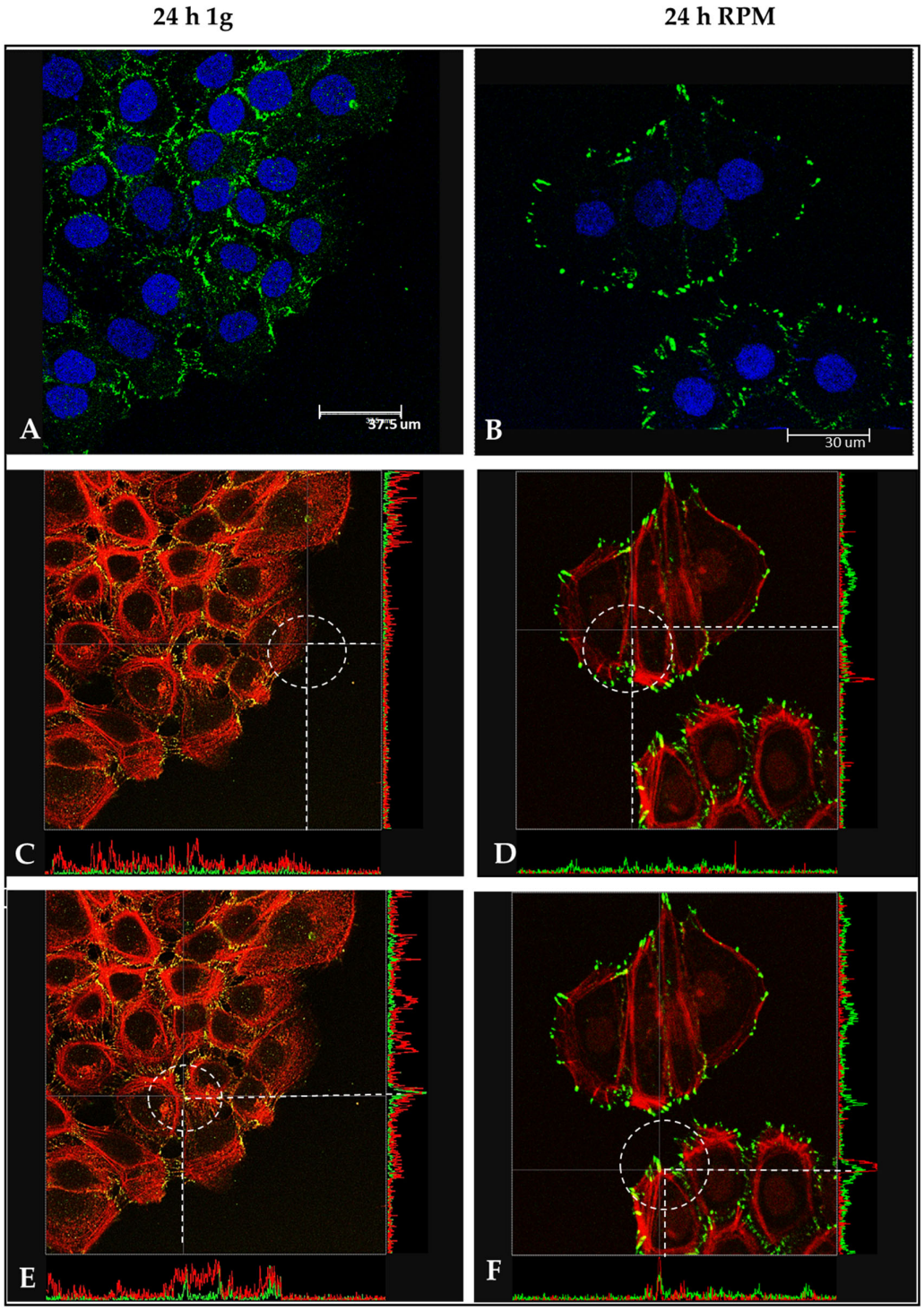

Figure 4. Representative images of colocalization analysis of vinculin (green) and F-actin (red) in HaCaT cells cultured in normal gravitational condition (1g) and microgravity conditions (RPM) for 24 h. In A, vinculin distribution is shown. Vinculin is distributed in cell–cell contact in control condition (**A**), (Scale bars 37.5 μm), while it is mostly displaced at the free front of cell membrane in RPM-treated cells (**B**) Scale bars 30 μm). (**C**–**F**) show the colocalization analysis of vinculin and F-actin. In the X/Y axes, at the level of the dotted lines, the colocalization (green and red picks) is shown. Colocalization is evident at the level of membrane protrusion in RPM cultured cells (**D**, dotted circle) and in cell–cell contact in 1g cultured cells (**E** dotted circle). Contrarily, no colocalization is observed at the level of membrane protrusion in on 1g cultured cells (**C**, dotted circle) and in cell–cell contact in RPM cultured cells (**F**, dotted circles).

3.2.2. F-Actin and Vinculin Organization at 48–72 h of Simulated Microgravity

To verify if the acquired phenotype at 24 h is stably maintained by cells exposed to microgravity, we extended the exposure times to 48 and 72 h. Surprisingly, after 48 h of simulated microgravity, lamellipodia and ruffles markedly decreased when compared to 24 h RPM cultured cells. After 72 h of microgravity exposition, the cytoskeleton architecture observed in the microgravity condition recovered almost completely the cytoskeleton organization usually observed in 1g control.

Specifically, by confocal analysis, we observed that after 48 h of microgravity, the exposition of vinculin at the cell periphery was appreciably diminished when compared to cells exposed for 24 h in weightlessness. Colocalization analyses demonstrated little or no colocalization (Figure 5C), although a good correlation with actin ($r = 0.92$; $p > 0.05$) can be recorded in few points. At cell-to-cell contact, colocalization with F-actin was observed (Figure 5E) and, as described in 1g treated samples, there is no significant positive relationship between the two markers ($r = 0.21$ $p > 0.05$).

After 72 h of microgravity exposition, the distribution of vinculin is almost concentrated within the areas of cell-to-cell contact, in which it shows a striking colocalization with F-actin bundles (Figure 5D,F), while little or no colocalization was observed in cell membranes at the leading edge of culture. Correlation analyses of vinculin with actin at the leading edge of the cell culture and in cell–cell contact showed no significant positive relationships ($r = 0.173$ $p > 0.05$; $r = 0.57$ $p > 0.05$ respectively), as we observed in the control condition.

Overall, these findings witness that after longer periods of microgravity exposure, cells recover their native phenotype, losing their migrating/invasive properties.

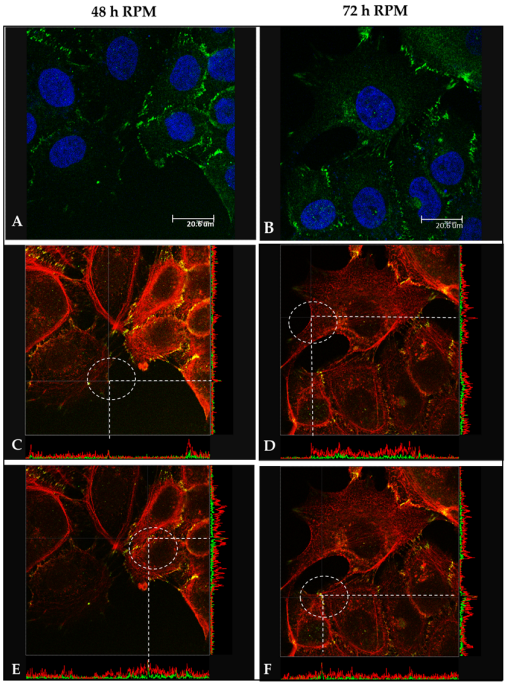

Figure 5. Representative images of colocalization analysis of vinculin (green) and F-actin (red) in HaCaT cells cultured in RPM for 48 and 72 h. In A, B vinculin distribution is shown; vinculin distribution is appreciably reduced at the cell periphery, while it is increased at the cell–cell contact both at 48 h (**A**) and 72 h (**B**). (**C**–**F**) show colocalization analysis of F-actin and vinculin. In the X/Y axes, at the level of the dotted lines, the colocalization (green and red picks) is shown. Colocalization after 48 h is still evident in some parts of the cellular periphery (**C**, dotted circle), albeit reduced compared to RPM at 24 h, and it appears in cell–cell contacts (**E**, dotted circle). Contrarily, at 72 h, no colocalization is observed at the level of periphery (**D**, dotted circle), while being recognizable in cell–cell contact areas (**F**, dotted circles). Scale bars 20.6 μm.

3.2.3. Reversibility of the Cytoskeleton Modifications

After 24 h of microgravity exposure, cells were replaced into a normal gravitational field, and cytoskeleton architecture was investigated after a further 24 h of 1g conditioning. Under these conditions, both F-actin filament organization and vinculin distribution recovered almost completely their normal distribution pattern. As shown in Figure 6, most of the cells reacquire a cortical F-actin organization as well as cell-to-cell contact of vinculin distribution, overlapping the picture observed in cells growing in 1g (Figure 6). Noticeably, F-actin and vinculin both colocalize mostly in proximity of cell-to-cell contact areas (Figure 6C). Correlation analyses of vinculin with F-actin at the leading edge of cell cultures and in cell–cell contact regions showed no significant positive relationship ($r = 0.218$, $p > 0.05$; $r = 0.465$, $p > 0.05$ respectively). These data demonstrate that the migratory phenotype acquired in the first 24 h in simulated microgravity conditions is almost completely reversed when cells are replaced into a normal gravity field.

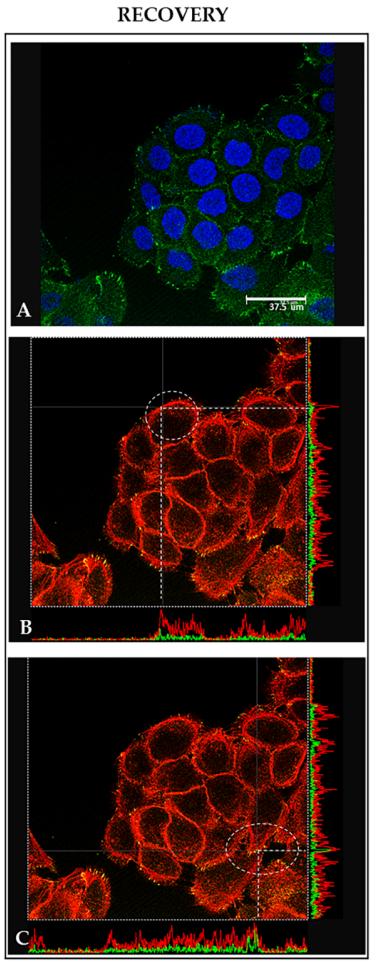

Figure 6. Representative images of colocalization analysis of vinculin (green) and F-actin (red) in HaCaT cells cultured in RPM for 24 h and then transferred into a normal gravitational field for a further 24 h (recovery conditions). In **A**, vinculin distribution is shown; vinculin recovers almost completely the distribution pattern observed in 1g cultured cells. (**B**,**C**) Colocalization analysis of F-actin and vinculin. In the X/Y axes, at the level of the dotted lines, the colocalization (green and red picks) is shown. Colocalization in the recovery condition appears mainly in cell–cell contacts (**C**, dotted circle), while none or little colocalization is observed at the level of the periphery (**B**, dotted circle). Scale bars: 37.5 μm.

3.3. Migration and Invasive Capability of HaCaT Exposed to Simulated Microgravity

To get insights into the migrating/invasive properties acquired by HaCaT cells exposed to microgravity for short periods, we planned specific experiments as previously described.

3.3.1. Cell Migration

Exposure to microgravity in RPM for 24 h strongly increases cell migration with respect to 1g control (3.44 ± 0.38 vs. 1.00 ± 0.17; $p < 0.01$), as observed in a preliminary study [11]. However, after 48 h of simulated microgravity, cell migration resulted significantly decreased when compared to 24-h RPM treated cells (1.95 ± 0.31 vs. 3.44 ± 0.3; $p < 0.05$). Yet, after 72 h of microgravity exposition, cell migration was further decreased, approaching values observed in 1g cultured cells (0.94 ± 0.14 vs. 1.00 ± 0.17; p = n.s.) (Figure 7A). Similar findings were obtained when HaCaT were replaced in 1g field for 24 h, after 24 h of weightlessness exposure. Indeed, the recovery experiment shows that cell migration was significantly reduced when compared to 24 h RPM-treated cells (1.28 ± 0.26 vs. 3.44 ± 0.38, §§ $p < 0.01$), whereas there was no significant difference with respect to 1g controls at 48 h (1.28 ± 0.26 vs. 1.00 ± 0.18 p = n.s.). In addition, no significant difference was observed with respect to cells maintained for 48 h in RPM condition (Figure 7 panel A and table).

3.3.2. Cell Invasiveness

In vitro invasion assay was performed using chambers coated with GFR Matrigel. As shown in Figure 7B, exposure to microgravity for 24 h strongly increases cell invasion with respect to 1g conditions (4.26 ± 0.66 vs. 1.00 ± 0.14; $p < 0.01$). To further confirm such behavior, we estimated by confocal microscopy the depth of Matrigel invasion reached by HaCaT cells exposed to microgravity for 24 h. As reported in Figure 8, HaCaT cells maintained at normal gravity form ovoidal structures and invade the matrix up to a depth of 49.71 ± 3.91 μm (Figure 8A–C), while cells growing in microgravity appear scattered and able to invade deeper, reaching a depth of 119.99 ± 5.67 μm ($p < 0.001$; Figure 8D–F). Overall, such findings confirm that cells exposed to microgravity for short periods dramatically increase their invasiveness capability

As noticed for cell migration, invasiveness decreases after 48 h of RPM with respect to 24-h RPM treated cells (2.91 ± 0.42 vs. 4.26 ± 0.66; $p < 0.05$). Moreover, after 72 h of microgravity exposition, cell invasion was significantly suppressed when compared to the 24 h RPM treated cells, (1.38 ± 0.08 vs. 4.26 ± 0.66; $p < 0.01$); HaCaT cells almost completely lose their invasive property, reaching values superimposable to those measured in 1g control cells (1.38 ± 0.08 vs. 1.00 ± 0.14 p = n.s.). Again, similar results were obtained when cells exposed to microgravity for 24 h were reseeded into a 1g field for 24 h: cells displayed significantly reduced invasiveness values in respect to the microgravity condition at 24 h (1.88 ± 0.31 vs. 4.26 ± 0.66 $p < 0.05$), the migrating phenotype "disappears", and cells recover values similar to those displayed by 1g controls at 48 h (1.88 ± 0.31 vs. 1.00 ± 0.19; p = n.s.). In addition, no significant difference was observed with respect to cells maintained for 48 h in RPM condition (Figure 7 panel B and table).

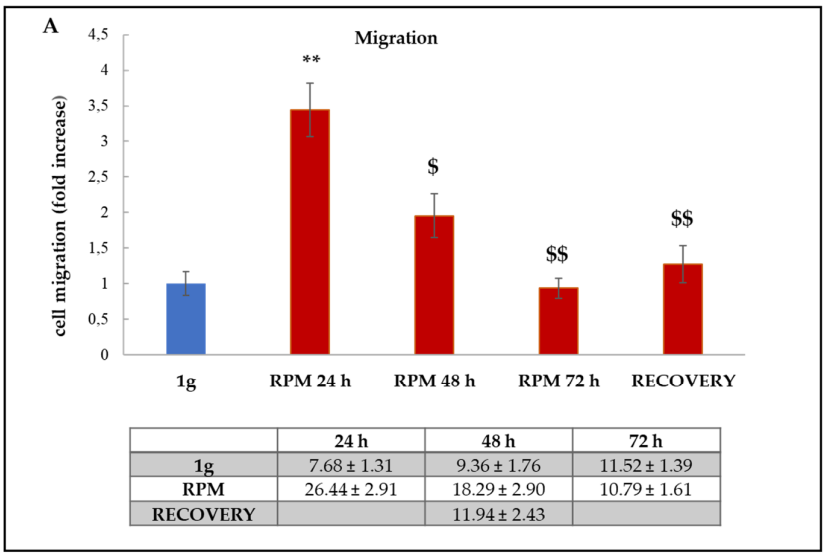

	24 h	48 h	72 h
1g	7.68 ± 1.31	9.36 ± 1.76	11.52 ± 1.39
RPM	26.44 ± 2.91	18.29 ± 2.90	10.79 ± 1.61
RECOVERY		11.94 ± 2.43	

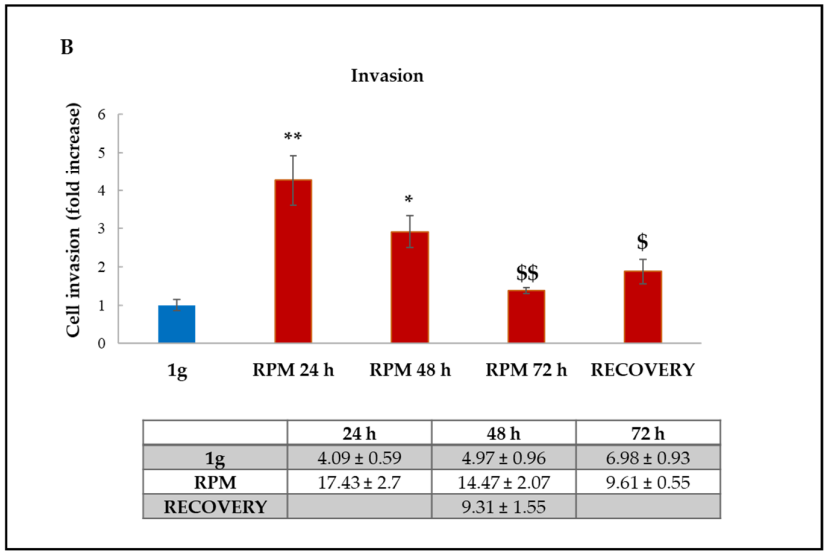

	24 h	48 h	72 h
1g	4.09 ± 0.59	4.97 ± 0.96	6.98 ± 0.93
RPM	17.43 ± 2.7	14.47 ± 2.07	9.61 ± 0.55
RECOVERY		9.31 ± 1.55	

Figure 7. Effect of microgravity exposure in RPM on migration (**A**) and invasion (**B**) in HaCaT cells. Data expressed as fold increase of control value considered as 1 are means of three independent experiments, each performed in quadruplicate, with S.D. represented by vertical bars (* $p < 0.05$; ** $p < 0.01$ versus 1g control; $^{\$}$ $p < 0.05$; $^{\$\$}$ $p < 0.01$ versus the cells exposed to RPM for 24 h by ANOVA followed by Bonferroni post-test). Tables illustrate the number of migrating and invading cells/field, respectively.

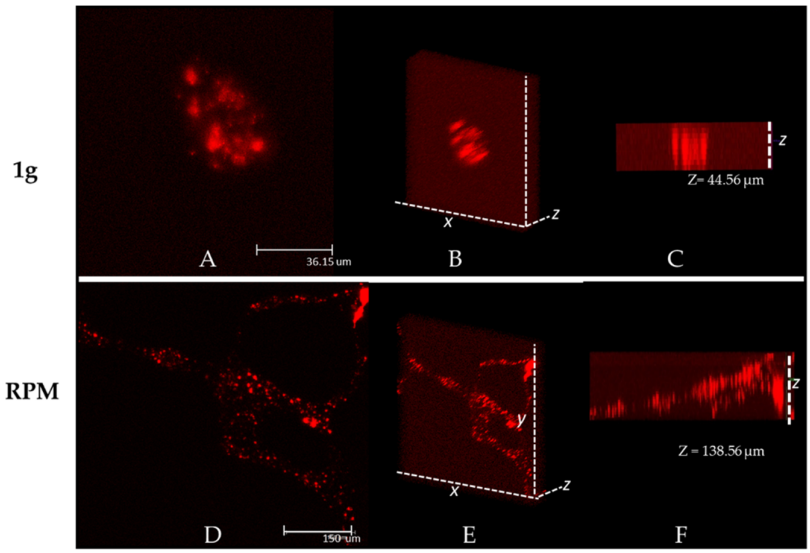

Depth z-axes (µm)	
1g	RPM
44.56	138.56
43.21	110.11
50.80	128.90
63.72	131.49
72.39	127.92
43.91	141.30
34.80	98.97
52.13	100.20
41.93	103.11
MEAN ± e.s.	
49.71 ± 3.91	119.99 ± 5.67

Figure 8. Representative images of Matrigel invasion by HaCaT after 24 h. HaCaT cells (red) were cultured on GFR Matrigel in normal gravitational condition (**A**–**C**, scale bar 7.5 µm) and microgravity conditions (**D**–**F**, scale bar 150 µm) for 24 h; (**A**,**D**) represent the confocal maximum projection; (**B**,**E**) represent 3D projection; (**C**,**F**) shows the depth analysis. As shown in this figure, HaCaT cells maintained at unit gravity invade matrix up to a depth of about 44.56 µm (**C**), while cells maintained in the microgravity condition are able to invade to a depth of about 138.56 µm (**F**). The table indicates the depth along the zeta axis measured in the three experiments performed (1g vs. RPM $p < 0.001$).

4. Discussion

HaCaT cells exposed to simulated microgravity show a biphasic response, displaying increased motility and invasiveness during the early period (24 h), which was followed by the recovering of a noninvasive morphological phenotype that is partly observed after 48 h and fully acquired at 72 h. Similar results were obtained by seeding again into a normal gravitational field those invasive HaCaT cells previously exposed to simulated microgravity for 24 h. Overall, these findings suggest that changes occurring at the morphological and functional level in cells exposed to microgravity for short periods have a transitory character and then are followed by adaptive modifications through which cells strive in recovering their native phenotype. Both E-cadherin and vinculin distribution patterns are likely to play a key role during those changes.

The actin ability to generate/transduce forces through cytoskeleton remodeling is a pivotal tool that enables cells in mechanosensing the environmental imbalance of physical forces. The transduction of mechanical stresses involves the clustering of transmembrane receptors that are instrumental in the successive assembly of focal contacts and adhesions that physically connect the extracellular matrix to the cell cytoskeleton [23]. Binding enhances the bundling of F-actin at the cell–substratum adhesion sites with the concomitant maturation of both the focal adhesions and the actin stress fibers [24], which represent mandatory steps to trigger the required tension for ensuring cell adherence and motility capability. It has been reported that exposure to microgravity reduces the number and total area of focal adhesions per cell [25], thus significantly reducing adherence to the substratum and migratory capability [26], albeit some contradictory results have been reported [27]. These changes are mandatory for the emergence of floating populations in cell cultures exposed to weightlessness, i.e., an organoid-like structure in which cells aggregate themselves after detaching from the substrate [28]. Therefore, our results are apparently at odds with those reported for other kind of cells. Differences in the experimental model, namely those involving different times of observation, can probably help in explaining this conundrum. Indeed, we observed increased motility only within the limited window of the first 24 h of microgravity exposure, given that after that time,

HaCaT cells progressively recovered the native phenotype, losing the invasive/motile phenotype. Moreover, effects of weightlessness on F-actin cytoskeleton are still a matter of debate. While a number of studies have reported that microgravity decreases F-actin expression, leading to disorganization of the cytoskeleton [29], other reports have reported opposite findings, with increased F-actin and stress fiber formation with the emergence of lamellipodia protrusions [30]. It is well known that vinculin has several effects on actin polymerization in newly formed adhesions. Vinculin can cross-link and bundle actin filaments, and it can recruit actin modifiers such as the Arp2/3 complex, which is a potent nucleator of actin polymerization. By contrast, vinculin and F-actin polymerization at cell–cell adhesions is less understood [18]. In our study, through analyzing the fluorescence intensity (SUM (I)) of actin and vinculin in cells exposed to simulated microgravity, we obtained a positive correlation between the two markers only at the level of newly formed FAs in cells cultured in the microgravity condition for 24 h. This correlation persists but decreases in membrane protrusions observed at 48 h of simulated microgravity, while at 72 h, it disappears and reaches values overlapping those observed in cells cultured in 1g. On the basis of these results, we can hypothesize that in the FAs that we observed and analyzed, vinculin is able to recruit actin filament within the FAs, while this phenomenon does not occur in cell–cell contact or in membrane protrusions of cells deprived of their migratory capability. Furthermore, in HaCaT cells cultured in RPM for 24 h and then transferred into a normal gravitational field for a further 24 h (recovery conditions), both F-actin filament and vinculin recovered almost completely the distribution and correlation pattern that we observed at 1g. All these data demonstrated that the emergence of FAs and consequently the F-actin remodeling occurring during the first 24 h should be considered a transient and adaptive phenomenon. Noticeably, these data outline that a critical factor in the emergence of the migrating/invasive phenotype is represented by the concomitant down-regulation of E-cadherin in cells exposed to microgravity for limited periods. Indeed, reduction in the expression pattern of E-cadherin during weightlessness indicated a transitory commitment toward an invasive phenotype, which is a critical feature that is also recorded in thyroid cancer cells exposed to short-term microgravity [30]. It is worth noting that the concomitant reduction in vinculin expression, which is witnessed by confocal studies during the first 24 h of microgravity exposure, can ultimately contribute in decreasing E-cadherin values, given that vinculin exerts a positive regulatory influence upon E-cadherin levels [31]. We hypothesize that the loosening of cell-to-cell adhesion, which is ascribed to reduced E-cadherin levels, plays a key role in favoring the emergence of a migratory/invasive phenotype despite the fact that the concomitant changes occurring in the cytoskeleton—i.e., the disorganization of F-Actin network and weakening of FA—would impair the migrating capability of HaCaT cells, at least in principle. This conclusion deserves to be emphasized, as it pinpoints E-cadherin as the pivotal factor that can switch cells toward a motile, invasive phenotype. Given that the metastatic potential of tumors is highly dependent on such capabilities, it is worth noting that the critical target of the treatment should be the restoration of proper E-cadherin values, as already underlined [32].

Loss of cell-to-cell adhesions is instrumental in enabling the disassembly of the cell cluster and in promoting their migratory capability. When and if such a condition persists, then organoid-like structures—in which cells are detached from the substratum and are recognizable as floating aggregates in the supernatant—appear [33]. In many microgravity-based models, the emergence of these organoid bodies is associated with the persistence of adherent cells, so it can be assumed that microgravity enacts the partitioning of living cells into two different populations, which is characterized by different morphological and functional properties [34]. However, by using the HaCaT model, we did not observe the formation of any organoid-like structure. On the contrary, these cells were shown to be able to counteract microgravity effects on both E-cadherin and F-actin, thus re-establishing a native, non-motile phenotype within 48–72 h of

adaptation in simulated microgravity. These results suggest that caution should be kept when considering data from weightlessness-based experiments, given that different exposure times can generate different biological behaviors. Overall, living cells seem to successfully cope with the microgravity challenge by enacting an "adaptive strategy", which mostly relies on the intrinsic plasticity of cells.

5. Conclusions

HaCaT cells exposed to simulated microgravity show a biphasic response, displaying increased motility and invasiveness during the early period (24 h), followed by the recovering of a noninvasive morphological phenotype at 48 and 72 h. Although changes in the cytoskeleton and F-actin organization would in principle inhibit the migrating capability of HaCaT cells by reducing cell adhesiveness to the substratum, the concomitant reduction in cell-to-cell adhesion fostered by the significant decrease in the E-cadherin expression pattern promoted the appearance of a migrating/invasive phenotype. However, those changes are transitory, and the native phenotype is re-established within 48–72 h in microgravity cultures. It is worthy of interest that the morphological recovery is paired by the concomitant disappearance of main EMT features. A similar pattern can be observed as the same cells are seeded again into a normal gravitational field. Definitely, the emergence of a migratory phenotype should be considered in this cellular model as a transient, adaptive phenomenon enacted by the modified environmental physical forces.

Further studies to elucidate the molecular mechanisms behind the morphological and functional changes we observed are currently undergoing in our laboratory.

Author Contributions: Conceptualization, A.C. (Angela Catizone), A.C. (Alessandra Cucina), G.R.; methodology, A.C. (Angela Catizone), A.C. (Alessandra Cucina), S.P., S.D., G.R., M.C.; software, A.C. (Angela Catizone), S.P., A.C. (Alessandra Cucina); validation, A.C. (Angela Catizone), A.C. (Alessandra Cucina), G.R.; formal analysis, A.C. (Angela Catizone), A.C. (Alessandra Cucina), G.R., F.F.; investigation, A.C. (Angela Catizone), A.C. (Alessandra Cucina), G.R., M.C.; data curation, A.C. (Angela Catizone), A.C. (Alessandra Cucina), A.F., S.P., G.R.; writing—original draft preparation, A.C. (Angela Catizone), A.C. (Alessandra Cucina); writing—review and editing, M.B., S.P., A.F., G,R.; visualization, A.F., G.R.; supervision, A.F., A.C. (Angela Catizone), M.B., project administration, A.C. (Angela Catizone), A.C. (Alessandra Cucina); funding acquisition, A.C. (Angela Catizone), F.F., G.R., A.C. (Alessandra Cucina). All authors have read and agreed to the published version of the manuscript.

Funding: This work was supported by Department of Experimental Medicine Università degli Studi della Campania "Luigi Vanvitelli" grant for researcher to Giulia Ricci (2015 and 2016). FFBAR 2017 to Giulia Ricci. ASI Contract to Giulia Ricci "Shape 2014-018-R.0" CUP F84G14000150005. Research grant from "Sapienza" University: ASI contract to Angela Catizone and to Alessandra Cucina "Epirepair 2014-010-R.0" CUP F84G14000070005. Research grant from "Sapienza" University to Angela Catizone n 2015-26A15LSAR. FFBAR 2017.

Acknowledgments: The authors wish to thank Prof. M.R. Torrisi, Sapienza University, Rome, Italy) to kindly provided human keratinocyte cell line HaCaT.

Conflicts of Interest: The authors declare no conflict of interest.

References

1. Pietsch, J.; Bauer, J.; Egli, M.; Infanger, M.; Wise, P.; Ulbrich, C.; Grimm, D. The effects of weightlessness on the human organism and mammalian cells. *Curr Mol. Med.* **2011**, *11*, 350–364, doi:10.2174/156652411795976600.
2. Masiello, M.G.; Cucina, A.; Proietti, S.; Palombo, A.; Coluccia, P.; D'Anselmi, F.; Dinicola, S.; Pasqualato, A.; Morini, V.; Bizzarri, M. Phenotypic switch induced by simulated microgravity on MDA-MB-231 breast cancer cells. *Biomed. Res. Int.* **2014**, *2014*, 652434, doi:10.1155/2014/652434.
3. Ferranti, F.; Caruso, M.; Cammarota, M.; Masiello, M.G.; Corano Scheri, K.; Fabrizi, C.; Fumagalli, L.; Schiraldi, C.; Cucina, A.; Catizone, A.; et al. Cytoskeleton modifications and autophagy induction in TCam-2 seminoma cells exposed to simulated microgravity. *Biomed. Res. Int.* **2014**, *2014*, 904396, doi:10.1155/2014/904396.

4. Pisanu, M.E.; Noto, A.; De Vitis, C.; Masiello, M.G.; Coluccia, P.; Proietti, S.; Giovagnoli, M.R.; Ricci, A.; Giarnieri, E.; Cucina, A.; et al. Lung cancer stem cell lose their stemness default state after exposure to microgravity. *Biomed. Res. Int.* **2014**, *2014*, 470253, doi:10.1155/2014/470253.
5. Wuest, S.L.; Richard, S.; Kopp, S.; Grimm, D.; Egli, M. Simulated microgravity: Critical review on the use of random positioning machines for mammalian cell culture. *Biomed. Res. Int.* **2015**, *2015*, 971474, doi:10.1155/2015/971474.
6. Clement, J.Q.; Lacy, S.M.; Wilson, B.L. Gene Expression Profiling of Human Epidermal Keratinocytes in Simulated Microgravity and Recovery Cultures. *Genom. Proteom. Bioinform.* **2008**, *6*, 8–28, doi:10.1016/s1672-0229(08)60017-0.
7. Ranieri, D.; Cucina, A.; Bizzarri, M.; Alimandi, M.; Torrisi, M.R. Microgravity influences circadian clock oscillation in human keratinocytes. *FEBS Open Bio* **2015**, *5*, 717–723, doi:10.1016/j.fob.2015.08.012.
8. Wong, V.W.; Longaker, M.T.; Gurtner, G.C. Soft tissue mechanotransduction in wound healing and fibrosis. *Semin Cell Dev. Biol.* **2012**, *23*, 981–986, doi:10.1016/j.semcdb.2012.09.010.
9. Mao, X.W.; Pecaut, M.J.; Stodieck, L.S.; Ferguson, V.L.; Bateman, T.A.; Bouxsein, M.L.; Gridley, D.S. Biological and metabolic response in STS-135 space-flown mouse skin. *Free Radic. Res.* **2014**, *48*, 890–897, doi:10.3109/10715762.2014.920086.
10. Neutelings, T.; Nusgens, B.V.; Liu, Y.; Tavella, S.; Ruggiu, A.; Cancedda, R.; Gabriel, M.; Colige, A.; Lambert, C. Skin physiology in microgravity: A 3-month stay aboard ISS induces dermal atrophy and affects cutaneous muscle and hair follicles cycling in mice. *NPJ Microgravity* **2015**, *1*, 15002, doi:10.1038/npjmgrav.2015.2.
11. Ranieri, D.; Proietti, S.; Dinicola, S.; Masiello, M.G.; Rosato, B.; Ricci, G.; Cucina, A.; Catizone, A.; Bizzarri, M.; Torrisi, M.R. Simulated microgravity triggers epithelial mesenchymal transition in human keratinocytes. *Sci. Rep.* **2017**, *7*, 538, doi:10.1038/s41598-017-00602-0.
12. Stone, R.C.; Pastar, I.; Ojeh, N.; Chen, V.; Liu, S.; Garzon, K.I.; Tomic-Canic, M. Epithelial-mesenchymal transition in tissue repair and fibrosis. *Cell Tissue Res.* **2016**, *365*, 495–506, doi:10.1007/s00441-016-2464-0.
13. Haensel, D.; Dai, X. Epithelial-to-mesenchymal transition in cutaneous wound healing: Where we are and where we are heading. *Dev. Dyn.* **2018**, *247*, 473–480, doi:10.1002/dvdy.24561.
14. Arnoux, V., C.C., Kusewitt DF, Hudson LG, Savagner, P. Cutaneous Wound Reepithelialization. In *Rise and Fall of Epithelial Phenotype*; Springer: Boston, MA, USA, 2005, doi:10.1007/0-387-28671-3_8.
15. Nieto, M.A.; Huang, R.Y.; Jackson, R.A.; Thiery, J.P. Emt: 2016. *Cell* **2016**, *166*, 21–45, doi:10.1016/j.cell.2016.06.028.
16. Andrews, J.P.; Marttala, J.; Macarak, E.; Rosenbloom, J.; Uitto, J. Keloids: The paradigm of skin fibrosis—Pathomechanisms and treatment. *Matrix Biol.* **2016**, *51*, 37–46, doi:10.1016/j.matbio.2016.01.013.
17. Wells, A.; Nuschke, A.; Yates, C.C. Skin tissue repair: Matrix microenvironmental influences. *Matrix Biol.* **2016**, *49*, 25–36, doi:10.1016/j.matbio.2015.08.001.
18. Bays, J.L.; DeMali, K.A. Vinculin in cell-cell and cell-matrix adhesions. *Cell Mol. Life Sci.* **2017**, *74*, 2999–3009, doi:10.1007/s00018-017-2511-3.
19. Grashoff, C.; Hoffman, B.D.; Brenner, M.D.; Zhou, R.; Parsons, M.; Yang, M.T.; McLean, M.A.; Sligar, S.G.; Chen, C.S.; Ha, T.; et al. Measuring mechanical tension across vinculin reveals regulation of focal adhesion dynamics. *Nature* **2010**, *466*, 263–266, doi:10.1038/nature09198.
20. Peng, X.; Nelson, E.S.; Maiers, J.L.; DeMali, K.A. New insights into vinculin function and regulation. *Int. Rev. Cell Mol. Biol.* **2011**, *287*, 191–231, doi:10.1016/B978-0-12-386043-9.00005-0.
21. Carisey, A.; Tsang, R.; Greiner, A.M.; Nijenhuis, N.; Heath, N.; Nazgiewicz, A.; Kemkemer, R.; Derby, B.; Spatz, J.; Ballestrem, C. Vinculin regulates the recruitment and release of core focal adhesion proteins in a force-dependent manner. *Curr. Biol.* **2013**, *23*, 271–281, doi:10.1016/j.cub.2013.01.009.
22. Morabito, C.; Guarnieri, S.; Catizone, A.; Schiraldi, C.; Ricci, G.; Mariggio, M.A. Transient increases in intracellular calcium and reactive oxygen species levels in TCam-2 cells exposed to microgravity. *Sci. Rep.* **2017**, *7*, 15648, doi:10.1038/s41598-017-15935-z.
23. Maniotis, A.J.; Chen, C.S.; Ingber, D.E. Demonstration of mechanical connections between integrins, cytoskeletal filaments, and nucleoplasm that stabilize nuclear structure. *Proc. Natl. Acad. Sci. USA* **1997**, *94*, 849–854, doi:10.1073/pnas.94.3.849.
24. Wolfenson, H.; Bershadsky, A.; Henis, Y.I.; Geiger, B. Actomyosin-generated tension controls the molecular kinetics of focal adhesions. *J. Cell Sci.* **2011**, *124*, 1425–1432, doi:10.1242/jcs.077388.
25. Tan, X.; Xu, A.; Zhao, T.; Zhao, Q.; Zhang, J.; Fan, C.; Deng, Y.; Freywald, A.; Genth, H.; Xiang, J. Simulated microgravity inhibits cell focal adhesions leading to reduced melanoma cell proliferation and metastasis via FAK/RhoA-regulated mTORC1 and AMPK pathways. *Sci. Rep.* **2018**, *8*, 3769, doi:10.1038/s41598-018-20459-1.
26. Dietz, C.; Infanger, M.; Romswinkel, A.; Strube, F.; Kraus, A. Apoptosis Induction and Alteration of Cell Adherence in Human Lung Cancer Cells under Simulated Microgravity. *Int. J. Mol. Sci.* **2019**, *20*, doi:10.3390/ijms20143601.
27. Shi, Z.X.; Rao, W.; Wang, H.; Wang, N.D.; Si, J.W.; Zhao, J.; Li, J.C.; Wang, Z.R. Modeled microgravity suppressed invasion and migration of human glioblastoma U87 cells through downregulating store-operated calcium entry. *Biochem. Biophys. Res. Commun.* **2015**, *457*, 378–384, doi:10.1016/j.bbrc.2014.12.120.
28. Po, A.; Giuliani, A.; Masiello, M.G.; Cucina, A.; Catizone, A.; Ricci, G.; Chiacchiarini, M.; Tafani, M.; Ferretti, E.; Bizzarri, M. Phenotypic transitions enacted by simulated microgravity do not alter coherence in gene transcription profile. *NPJ Microgravity* **2019**, *5*, 27, doi:10.1038/s41526-019-0088-x.
29. Corydon, T.J.; Kopp, S.; Wehland, M.; Braun, M.; Schutte, A.; Mayer, T.; Hulsing, T.; Oltmann, H.; Schmitz, B.; Hemmersbach, R.; et al. Alterations of the cytoskeleton in human cells in space proved by life-cell imaging. *Sci. Rep.* **2016**, *6*, 20043, doi:10.1038/srep20043.

30. Nassef, M.Z.; Kopp, S.; Wehland, M.; Melnik, D.; Sahana, J.; Kruger, M.; Corydon, T.J.; Oltmann, H.; Schmitz, B.; Schutte, A., et al. Real Microgravity Influences the Cytoskeleton and Focal Adhesions in Human Breast Cancer Cells. *Int. J. Mol. Sci.* **2019**, *20*, doi:10.3390/ijms20133156.
31. Hazan, R.B.; Kang, L.; Roe, S.; Borgen, P.I.; Rimm, D.L. Vinculin is associated with the E-cadherin adhesion complex. *J. Biol. Chem.* **1997**, *272*, 32448–32453, doi:10.1074/jbc.272.51.32448.
32. Chen, H.; Paradies, N.E.; Fedor-Chaiken, M.; Brackenbury, R. E-cadherin mediates adhesion and suppresses cell motility via distinct mechanisms. *J. Cell Sci.* **1997**, *110*, 345–356.
33. Costantini, D.; Overi, D.; Casadei, L.; Cardinale, V.; Nevi, L.; Carpino, G.; Di Matteo, S.; Safarikia, S.; Valerio, M.; Melandro, F., et al. Simulated microgravity promotes the formation of tridimensional cultures and stimulates pluripotency and a glycolytic metabolism in human hepatic and biliary tree stem/progenitor cells. *Sci. Rep.* **2019**, *9*, 5559, doi:10.1038/s41598-019-41908-5.
34. Masiello, M.G.; Verna, R.; Cucina, A.; Bizzarri, M. Physical constraints in cell fate specification. A case in point: Microgravity and phenotypes differentiation. *Prog. Biophys. Mol. Biol.* **2018**, *134*, 55–67, doi:10.1016/j.pbiomolbio.2018.01.001.